Neuropathy Target Esterase Is Degraded by the Ubiquitin–Proteasome Pathway with ARA54 as the Ubiquitin Ligase

Ding-Xin Long,[†,‡] Pan Wang,[†] Ying-Jian Sun,[†,§] Rui Chen,[†] and Yi-Jun Wu*[,†]

[†]Laboratory of Molecular Toxicology, State Key Laboratory of Integrated Management of Pest Insects and Rodents, Institute of Zoology, Chinese Academy of Sciences, Beijing 100101, P. R. China
[‡]School of Public Health, University of South China, Hengyang 421001, P. R. China
[§]Department of Veterinary Medicine and Animal Science, Beijing Agriculture College, Beijing 102206, P. R. China

ABSTRACT: Neuropathy target esterase (NTE) is an endoplasmic reticulum membrane-associated phospholipase B, which is essential for embryonic and nervous system development. However, the regulation of NTE at the protein level had not been thoroughly investigated. Our previous study showed that NTE was degraded not only by the macroautophagy–lysosome pathway but also by the ubiquitin–proteasome pathway. Here we further reveal that androgen receptor-associated protein 54 (ARA54) regulated the ubiquitin–proteasome degradation of NTE. We find that deletion of the regulatory domain of NTE, which possesses a putative destruction box and thus is essential for its degradation by the proteasome, prevented its degradation by the proteasome. In addition, we demonstrate that ARA54, which has a RING finger domain and E3 ligase activity, interacts directly with NTE. Overexpression of ARA54 downregulates the protein level of NTE, and knockdown of ARA54 inhibits the degradation of NTE. The mutation in the RING domain of ARA54 blocks the degradation of NTE by ARA54, which indicates that the RING domain is essential for ARA54's E3 activity. These findings suggest that ARA54 acts as the ubiquitin ligase to regulate the ubiquitin–proteasome degradation of NTE.
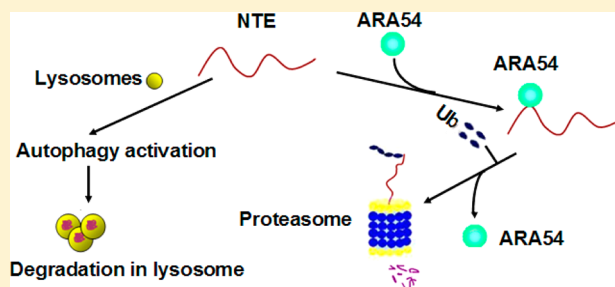
Neuropathy target esterase (NTE) was initially identified as the primary target protein of certain neurotoxic organophosphorus compounds (OPs).[1] The inhibition of NTE by OPs triggers a delayed neuropathy (OPIDN) characterized by demyelination and degeneration of long nerve axons in humans, and laboratory animals.[2,3] NTE is critical for normal embryonic and nervous system development. In mice, complete inactivation of the NTE gene results in embryonic lethality because of placental failure and impaired vasculogenesis,[4,5] while mice with a brain-specific deletion of NTE exhibit neurodegeneration.[6] Moreover, a recent finding has shown that mutations in NTE cause motor neuron disease.[7]

NTE is a 1327-amino acid polypeptide with two functional domains, an amino-terminal putative regulatory domain of ∼700 residues containing three speculated cyclic nucleotide-binding domains and a carboxyl-terminal catalytic/esterase domain that includes a patatin domain (Figure 1A).[8] NTE is anchored to the cytoplasmic face of the endoplasmic reticulum (ER) by an amino-terminal transmembrane segment (TM), and the regulatory and catalytic domains interact with the cytoplasmic face of the ER.[6,8] Previous observations indicate that NTE displays potent lysophospholipase activity in the mouse brain.[9] Further characterization of this activity shows that it is responsible for converting phosphatidylcholine to glycerophosphocholine in mammalian cells and regulating phosphatidylcholine homeostasis in *Drosophila*.[10,11]
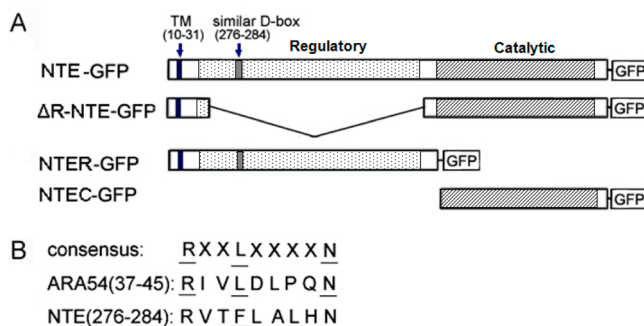

Figure 1. NTE constructs used in this study and the D-box sequence in NTE and ARA54. (A) Full-length NTE (1327 amino acids) (NTE) and three truncated NTE forms [ΔR-NTE (Δ158–673), NTER (1–680), and NTEC (681–1307)] were tagged with GFP at the carboxyl terminus. The predicted TM (10–31) is represented with blue vertical lines, and the position of the proposed D-box site (276–284) is indicated by an arrow. The putative regulatory domain (R) and the catalytic domain (C) are shown as red and yellow areas, respectively. (B) Sequence comparison of the D-box in NTE and ARA54. Similar sites are indicated by underlining.

Although the character and function of NTE have been elucidated, the regulation of NTE is still not completely known. NTE may be controlled by protein kinase C (PKC) because it is downregulated by PKC activator phorbol 12-myristate 13-acetate (PMA) in a manner blocked by PKC inhibitor staurosporine.[12] There is a direct interaction between NTE and G protein β-2, which may regulate NTE activity.[13] Our previous results show that NTE was degraded by the macroautophagic lysosomal pathway.[14] Preliminary bioinformatics analysis of the NTE sequence shows that there is a sequence (R-V-T-F-L-A-L-H-N, amino acids 276−284) similar to the destruction box (D-box) composed of the sequence R-X-X-L-X-X-X-X-N within the putative regulatory domain (Figure 1B). The D-box is a known recognition signal found in substrates that are degraded by the ubiquitin (Ub)−proteasome pathway (UPP).[15,16] Thus it suggests that the UPP is involved in the degradation of NTE. Indeed, our recent study showed that NTE accumulated in the cells after treatment with proteasome inhibitor epoxomicin,[17] indicating that the proteasome was involved in NTE degradation.

The Ub−proteasome system plays a central role in selective protein degradation in eukaryotic cells and is involved in a variety of cellular functions.[18] Ubiquitination of a target protein requires sequential reactions involving three types of enzymes, Ub-activating enzyme (E1), Ub-conjugating enzyme (E2), and Ub-ligase (E3). E3s play important roles in catalyzing the formation of Ub chains on the substrate. A number of RING (really interesting new gene)-finger proteins have been identified to directly bind their substrates and exhibit E3 activity.[19,20] Androgen receptor (AR)-associated protein 54 (ARA54) was demonstrated to have the RING domain and E3 ligase activity.[18]

In our early study, we identified ARA54 as an interacting protein with NTE by using yeast two-hybrid screening.[21] In the study presented here, we first demonstrated that NTE's regulatory domain was critical for its degradation by UPP. Then, we showed that ARA54 could regulate the level of NTE as an Ub-ligase. These findings suggest that multiple pathways could regulate NTE at the protein level.

■ MATERIALS AND METHODS

Materials. The pNTE-GFP, pΔTM-NTE-GFP, and D16 plasmids containing the full-length cDNA sequence of human NTE were generous gifts from P. Glynn's lab (Toxicology Unit, MRC, U.K.).[8] Plasmid pMT132 (HA-tagged Ub) and plasmids pACT2-ARA54 and pACT2-mtARA54 were kindly donated by D. Bohmann (University of Rochester, Rochester, NY) and Y. Okano (Gifu University School of Medicine, Gifu, Japan), respectively. Cell culture reagents, cycloheximide, lactacystin, MG132, 3-methyladenine (3-MA), and anti-ARA54 antibody were purchased from Sigma-Aldrich (St. Louis, MO), and the transfection reagent VigoFect was purchased from Vigorous Biotechnology (Beijing, China). Human NTE-specific antibody against peptides corresponding to amino acids 1316−1327 (LPQEPPGSATDA) was generated by Beijing B&M Biotech Co. Ltd. (Beijing, China). Mouse anti-Myc monoclonal antibody, mouse anti-ARA54 monoclonal antibody, rabbit anti-ubiquitin polyclonal antibody, rabbit anti-actin polyclonal antibody, mouse anti-GFP monoclonal antibody, mouse anti-HA monoclonal antibody, goat anti-mouse IgG HRP, and goat anti-rabbit IgG HRP were purchased from Santa Cruz Biotechnology (Santa Cruz, CA). Enhanced chemilumines-

cence (ECL) reagents were obtained from Applygen Technologies Inc. (Beijing, China).

Plasmid Construction. To generate the expression constructs of ARA54 and mutant ARA54 (mtARA54) with Myc tag pCMV-Myc-ARA54 and pCMV-Myc-mtARA54, the full-length coding cDNA sequences for ARA54 and mtARA54 were amplified from pACT2-ARA54 and pACT2-mtARA54, respectively, using primers 5′-CGGAATTCGGATGTCGTC-AGAAGATCGAGAA-3′ and 5′-CTCTCGAGCTAGTCTTC-TACCTCATCTTC-3′. The polymerase chain reaction (PCR) products were inserted into *Eco*RI and *Xho*I sites of pCMV-Myc vectors. Both constructs were confirmed by sequencing.

For generating an ARA54-DsRed fusion construct, the ARA54 coding sequence was amplified using two specific primers: a forward primer containing an internal *Eco*RI site (5′-CGGAATTCGCCATGTCGTCAGAAGATCGAGAA-3′) and a reverse primer including a *Bam*HI site (5′-CTGGATCCG-GGTCTTCTACCTCATCTTCCCA-3′). PCR production was cloned into the *Eco*RI and *Bam*HI sites of the vector pDsRed1-N1 to make ARA54-DsRed, confirmed by DNA sequencing. Plasmids pNTER-GFP and pNTEC-GFP were generated in our laboratory.[14]

Cell Culture, Transfection, and Treatments. Human neuroblastoma cell line SH-SY5Y and HeLa cancer cell lines were obtained from the Cell Center of the Chinese Academy of Medical Sciences (Beijing, China). Monkey kidney COS7 cells were kindly provided by Y.-L. Wang (State Key Lab of Reproductive Biology, Beijing, China). SH-SY5Y, HeLa, and COS-7 cells were maintained in Dulbecco's modified Eagle's medium (Sigma) supplemented with 10% fetal calf serum and 100 units of penicillin-streptomycin. Incubations were conducted at 37 °C in a humidified 5% CO_2/95% air atmosphere. Cell transfection was performed according to the manual of the Vigorous transfection reagent. After transfection for 24 h, MG132 or lactacystin dissolved in dimethyl sulfoxide (DMSO) was added to inhibit the protein degradation by UPP, and DMSO treatment was the control. At the same time, 30 μM cycloheximide was added to the cells to avoid the confounding effects of ongoing protein synthesis. The cell lysates and protein samples were prepared, and Western blotting was performed according to the method described in ref 14. The blots were stripped and reprobed for anti-actin antibody if needed. Densitometry of Western blotting was conducted using ImageJ.

Co-immunoprecipitation Assays. COS7 cells were transfected with pNTE-EGFP (pEGFP-N3 vector as a control) and pMT123 (HA-Ub) or pCMV-Myc-ARA54 vector by the Vigorous transfection reagent. Forty-eight hours later, the cells were rinsed three times with ice-cold PBS and lysed in lysis buffer [50 mM Tris (pH 7.5), 1% NP-40, 0.5% Na_3VO_4, 150 mM NaCl, and 1 mM EDTA]. For immunoprecipitation, the cell lysates were incubated with primary antibody and rotated at 4 °C for 3 h. Protein A/G agarose (Santa Cruz Biotechnology) beads were used to immobilize antibody-bound proteins. Immunoprecipitates were washed three times with lysis buffer and resuspended in sodium dodecyl sulfate−polyacrylamide gel electrophoresis loading buffer for immunoblotting analysis.

Fluorescence Microscopy. COS7 cells were seeded on the coverslips in six-well plates for fluorescence analysis. Twenty-four hours after being seeded, the cells were cotransfected to express NTE-GFP and ARA54-DsRed. Forty-eight hours after transfection, the cells were washed three times with Tris-buffered saline {TBS [50 mM Tris-HCl and 150 mM NaCl
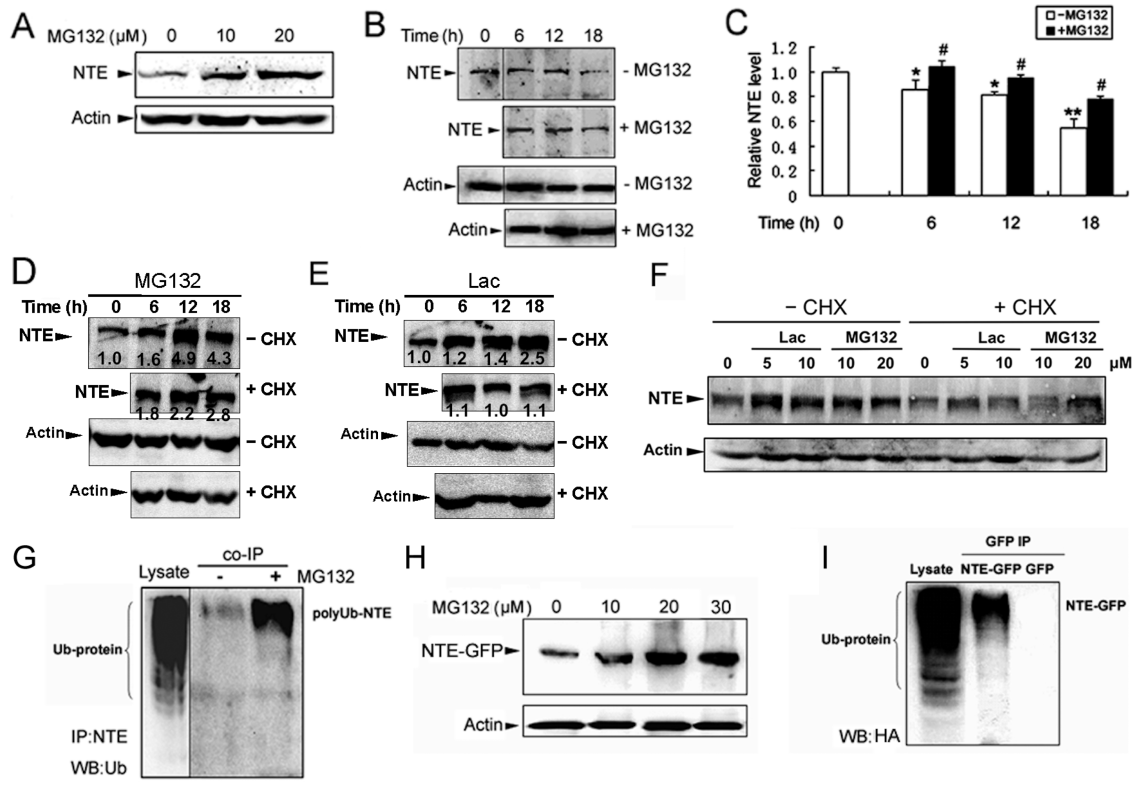
Figure 2. Proteasome inhibitor treatment promoted NTE accumulation, and NTE was modified by ubiquitination. (A) SH-SY5Y cells were treated for 18 h with different concentrations of MG132 and then lysed. Total cell lysates were analyzed by immunoblotting using anti-NTE antibody. Actin was used as a loading control. (B) SH-SY5Y cells were treated with or without 20 μM MG132 in the presence of 30 μM cycloheximide for the indicated time and lysed. Total cell lysates were analyzed by immunoblotting using anti-NTE antibody. Actin was used as a loading control. (C) Relative levels of NTE (fold of 0 h control) in the presence (■) or absence (□) of MG132 quantified by densitometry. Data are expressed as the means $\pm$ SE ($n = 3$). Asterisks indicate effects significantly different from control (0 h): *$P < 0.05$, **$P < 0.01$; # indicates a significant difference between groups in the presence of MG132 and absence of MG132 in the indicated time ($P < 0.05$). (D) HeLa cells were treated with or without 30 μM cycloheximide (CHX) in the presence of 20 μM MG132 for the indicated time and lysed. Total cell lysates were analyzed by immunoblotting using anti-NTE antibody. The number under each NTE band showed the relative level of NTE to actin quantified by densitometry. Actin was used as a loading control. (E) HeLa cells were treated with or without 30 μM cycloheximide (CHX) in the presence of 10 μM lactacystin (Lac) for the indicated time and lysed. Total cell lysates were analyzed by immunoblotting using anti-NTE antibody. The number under each NTE band shows the relative level of NTE to actin quantified by densitometry. Actin was used as a loading control. (F) HeLa cells were treated with or without 30 μM cycloheximide (CHX) in the presence of 5 or 10 μM lactacystin (Lac) or 10 or 20 μM MG132 for 18 h and lysed. Total cell lysates were analyzed by immunoblotting using anti-NTE antibody. Actin was used as a loading control. (G) SH-SY5Y cells were treated for 24 h with or without 10 μM MG132. Immunoprecipitation (IP) was performed with anti-NTE antibodies (IP: NTE), followed by immunoblotting (IB) with anti-ubiquitin antibodies (IB:Ub). The blots shown are representative of three independent experiments. (H) NTE-GFP-transfected COS7 cells were treated for 18 h with different concentrations (micromolar) of MG132 in the presence of 30 μM cycloheximide. Cell lysates were subjected to immunoblotting with anti-GFP antibodies. Actin was used as a loading control. (I) Polyubiquitination of NTE-GFP. COS7 cells were cotransfected with NTE-GFP and HA-Ub. After transfection for 48 h, cells were lysed in CHAPS buffer and co-IP of NTE-GFP and HA-Ub was performed using an anti-GFP monoclonal antibody. The co-immunoprecipitated NTE-GFP was detected by Western blotting using an anti-HA monoclonal antibody. The high-molecular weight smear indicates the polyubiquitinated NTE-GFP complex. The blots shown are representatives of three independent experiments. In Western blotting results, NTE protein was 155 kDa, actin protein was 42 kDa, and NTE-GFP was 182 kDa.

(pH 7.4)]}, then fixed with ice-cold 90% (v/v) methanol in TBS at −20 °C for 20 min, and washed with TBS twice. The distribution of NTE-GFP and ARA54-DsRed in cells was observed under a laser scanning confocal microscope (LSM510, Carl Zeiss, Jena, Germany). GFP and DsRed cotransfected cells were used as a control.

RNA Interference (RNAi) Experiments. Small interfering RNA (siRNA) target sites within the ARA54 gene were selected according to the method described in a previous study.[22] The siRNA inserts, containing selected 19-nucleotide coding sequences, followed by a nine-nucleotide spacer, an inverted repeat of the coding sequence, and five Ts, were generated as double-stranded DNAs with BamHI and HindIII sites and then cloned into plasmid pGenesil-1. The

corresponding oligos for generating ARA54 siRNA were 5′-*GATCCCCATGCCTCAACTGCCCAGAATTCAAGAGATT-CTGGGCAGTTGAGGCATTTTTTGGAAA*-3′ and 5′-*AGC-TTTTCCAAAAAATGCCTCAACTGCCCAGAATCTCTTG-AATTCTGGGCAGTTGAGGCATGGG*-3′. A nonfunctional scrambled siRNA was constructed as a negative control, which contains nucleotide substitutions at the 19-nucleotide targeting sequence of shRNA. The corresponding oligos for generating this scrambled siRNA control were 5′-*GATCCCCGATACG-AATTCAGACCGTATTCAAGAGATACGGTCTGAATTC-GTATCATTTTTGGAAA*-3′ and 5′-*AGCTTTTCCAAAAAG-ATACGAATTCAGACCGTATCTCTTGAATACGGTCTG-AATTCGTATCAGGG*-3′. Both constructs were verified by DNA sequencing. These constructs and mock plasmids were

transfected into HeLa cells by the Vigorous transfection reagent. After transfection for 48 h, cells were lysed to detect the expression of ARA54 and NTE by Western blotting analysis.

Statistical Analysis. Data were generally expressed as means ± the standard error. Groups of data were compared by one-way analysis of variance. A difference between means was considered significant when $P < 0.05$.

■ RESULTS

NTE and GFP-Tagged NTE Are Degraded by UPP. To determine whether NTE is degraded by the proteasome pathway, we assessed the effect of MG132, a widely used proteasome inhibitor,[23] on NTE protein clearance in human neuroblastoma cell line SH-SY5Y cells, which have high levels of NTE expression.[24] The NTE protein level was significantly increased by MG132 treatment at two different concentrations (10 and 20 μM) for 18 h in SH-SY5Y cells (Figure 2A). As shown in Figure 2B, in the presence of protein synthesis inhibitor cycloheximide (CHX), the protein level of human NTE decreased 43% within 18 h, while the degradation of NTE was suppressed by MG132 treatment (Figure 2C). In addition, when CHX was present, the increase in NTE by MG132 and another proteasome inhibitor lactacystin (Lac) treatment was inhibited (Figure 2D−F). Taken together, these results indicate that endogenous NTE is degraded by the proteasome.

Efficient recognition and degradation of ubiquitinated proteins by the proteasome requires addition of at least four ubiquitin residues to target proteins.[19] To determine whether NTE protein is ubiquitinated prior to its degradation by the proteasome, we performed immunoprecipitation assays. SH-SY5Y cells were treated with or without MG132 for 18 h, and the cell lysates were immunoprecipitated with anti-NTE antibody followed by immunoblotting with anti-ubiquitin antibody to detect polyubiquitinated NTE proteins. Poly-ubiquitinated forms of NTE were detected only in immunoprecipitated samples from cells after MG132 treatment, not cells without MG132 treatment (Figure 2G). These results demonstrate that some endogenous NTE proteins are ubiquitinated.

Furthermore, we observed protein clearance of NTE in COS7 cells transfected with GFP-tagged NTE in the presence of CHX (Figure 2H). As shown in Figure 2H, MG132 treatment significantly increased NTE-GFP levels in a dose-dependent manner, indicating that proteasome inhibitor MG132 prevents the degradation of NTE-GFP. However, when we transfected cells with GFP empty vector, we showed that GFP levels were basically not affected by MG132 treatment, which indicates that the proteasomal degradation is specific to NTE (data not shown). To determine whether the degradation of NTE-GFP by the proteasome is associated with ubiquitination, we performed co-immunoprecipitation to detect the polyubiquitinated NTE. Polyubiquitinated forms of NTE were detected in transfected COS7 cells expressing both NTE-GFP and HA-Ub, but not in cells transfected with HA-Ub and GFP (Figure 2I). These experiments were performed without Ub-conjugating enzyme (E2) or Ub-ligase transfection, indicating that endogenous E2 and E3 are sufficient to catalyze the ubiquitination reaction in COS7 cells.

NTE's Regulatory Domain (R) Contributes to Degradation of NTE by UPP. To further investigate whether the putative regulatory domain (R) or the hydrophobic catalytic domain (C) is involved in NTE degradation by UPP, three

truncated NTE forms (ΔR-NTE, NTER, and NTEC) tagged with GFP were also used for experiments. As expected, inhibition of UPP by MG132 for 18 h resulted in an obvious increase in the levels of NTER-GFP in the presence of cycloheximide. In contrast, the levels of ΔR-NTE-GFP and NTEC-GFP were not affected by MG132 treatments (Figure 3). These results indicate that the R domain of NTE, rather
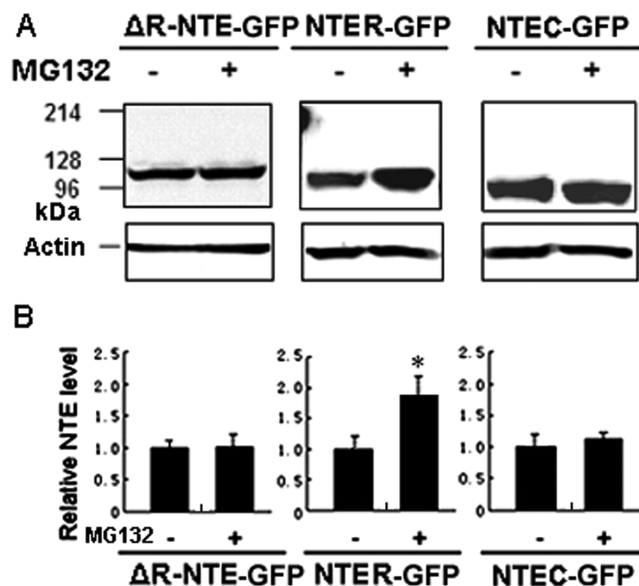

Figure 3. Proteasome inhibitor treatment promotes NTER-GFP accumulation. (A) COS7 cells were transiently transfected with the truncated forms (ΔR-NTE-GFP, NTER-GFP, and NTEC-GFP) of NTE. Twenty-four hours after transfection, cells were incubated with or without 20 μM MG132 in the presence of 30 μM cycloheximide for 18 h. Total cell lysates were analyzed by immunoblotting using anti-GFP antibody. Actin was used as a loading control. (B) The relative level of NTE was quantified by densitometry. Data are presented as means ± SE ($n = 3$). *$P < 0.05$.

than the TM domain and the C domain, contributes to NTE degradation by UPP and D-box may be located in the R domain of NTE.

NTE Is Degraded by the Proteasome Pathway and Macroautophagy. Our previous results showed that NTE was also degraded by macroautophagy.[14] We then assessed whether NTE was degraded by both pathways. HeLa cells were incubated with or without 10 mM 3-MA, 20 μM MG132, or 10 mM 3-MA with 20 μM MG132 in the presence of 30 μM cycloheximide for 18 h. Total cell lysates were analyzed by immunoblotting with anti-GFP antibody to detect the level of NTE. As shown in Figure 4, the protein levels of NTE in 3-MA-treated cells and MG132-treated cells increased compared with those of control cells. A further increase in the level of NTE was detected in cells cotreated with 3-MA and MG132 compared with that of 3-MA-treated cells or MG132-treated cells. These data further support the idea that NTE proteins are degraded by both macroautophagy and the proteasome.

NTE Directly Interacts with ARA54. To confirm the interaction between NTE and ARA54 in mammalian cells, co-immunoprecipitation assays were conducted. Myc-tagged ARA54 together with NTE-GFP (GFP as a control) was transfected into COS7 cells. Cell lysates were immunoprecipitated with anti-GFP antibody followed by immunoblotting with anti-Myc antibody. As shown in panels A and B of Figure 5,
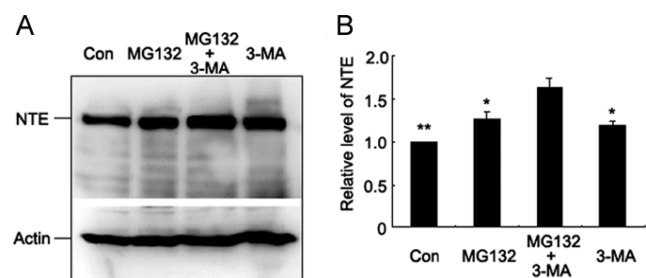
Figure 4. NTE is degraded by both the proteasome pathway and macroautophagy. (A) HeLa cells were incubated with or without 10 mM 3-MA, 20 μM MG132, or both inhibitors (10 mM 3-MA and 20 μM MG132) in the presence of 30 μM cycloheximide for 18 h. Total cell lysates were analyzed by immunoblotting with anti-GFP antibody. Actin was used as a loading control. (B) The relative level of NTE was quantified by densitometry. Data are presented as means $\pm$ SE ($n = 3$). *$P < 0.05$; **$P < 0.01$ in comparison with 3-MA with MG132 (analysis of variance with Dunnett's multiple-comparison test) . In Western blotting results, NTE protein was 155 kDa and actin protein was 42 kDa.

when NTE-GFP or ARA54 was immunoprecipitated from cell lysates, ARA54 or NTE was also precipitated, respectively. To determine whether endogenous NTE can form a complex with ARA54, co-immunoprecipitation assays were performed with HeLa cell lysates. We detected ARA54 protein when using an anti-NTE antibody to immunoprecipate NTE-interacting proteins (Figure 5D). These data confirm the physical interaction between NTE and ARA54 proteins in mammalian cells.

As fusion constructs containing GFP or red fluorescent proteins (DsRed) have been successfully used to detect the subcellular localization of numerous proteins,[25,26] we used GFP or DsRed fusion proteins to examine the location of ARA54 and NTE in individual living cells. GFP and ARA54-DsRed were found to be expressed ubiquitously in the cytoplasm and in the nucleus (Figure 5C, top panel), which was consistent with previous results.[27] Previous studies have shown that NTE is anchored in ER membranes, and overexpression of NTE can induce the aggregation of ER membranes in COS7 cells.[9] We observed green fluorescence that was seen only in the cytoplasm of NTE-GFP-expressing cells. NTE-GFP expression induced the aggregation of ARA54-DsRed (Figure 5C, bottom panel), indicating NTE-GFP colocalized with ARA54-DsRed. These results further demonstrate that the NTE and ARA54 proteins directly interact.

ARA54 Acts as Ub-Ligase To Regulate the Protein Level of NTE. To further investigate the role of ARA54 in the regulation of the NTE protein level, we overexpressed Myc-tagged ARA54 in HeLa cells. Overexpression of ARA54 significantly decreased the levels of NTE in HeLa cells (Figure 6A). However, the mRNA level of NTE was not changed in ARA54-expressing cells (data not shown). When ARA54-overexpressing HeLa cells were treated with MG132 or CHX, the increase or decrease in the NTE level was not as evident as in normal HeLa cells (Figure 6B) because the ARA54 level was induced by MG132 treatment and reduced by CHX treatment (Figure 6B). Thus, the level of degradation of NTE was higher after MG132 treatment and lower after CHX treatment compared to the level of NTE in cells without ARA54 expression. Therefore, the extent of accumulation of NTE was lower after MG132 treatment and higher after CHX treatment in cells with ARA54 expression than in NTE in cells without
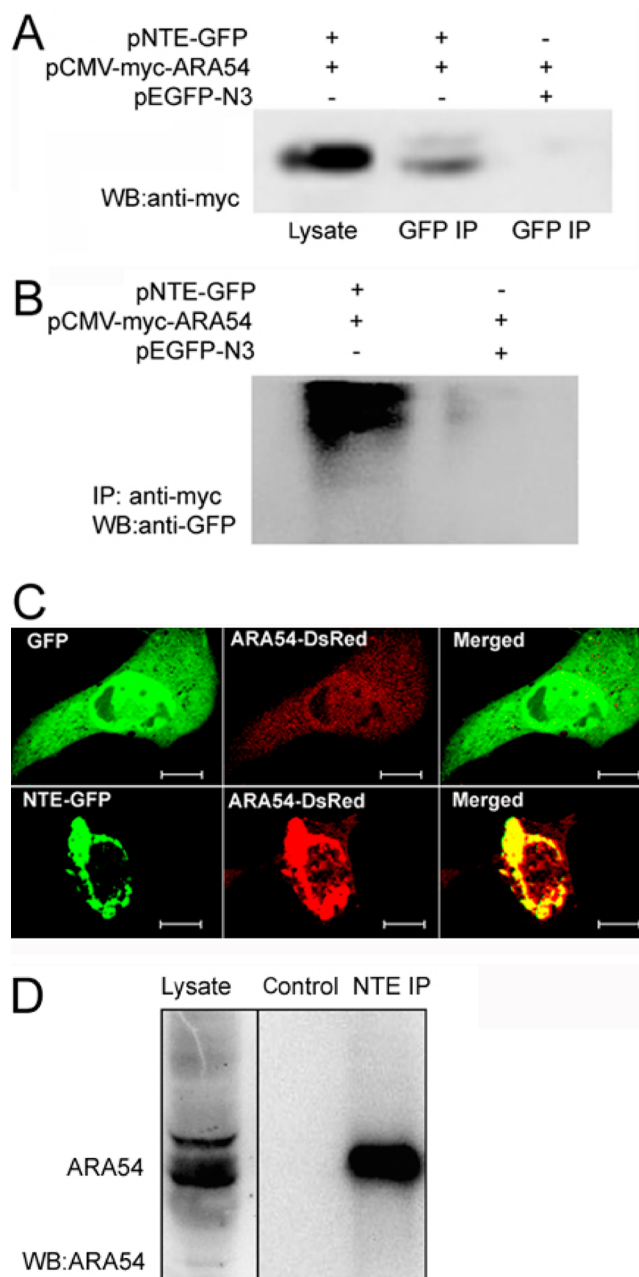

Figure 5. ARA54 interacts directly with NTE. (A) Co-immunoprecipitation confirms the interaction of ARA54 and NTE. COS7 cells were cotransfected with NTE-GFP (or GFP) and Myc-ARA54 as described in Materials and Methods. Forty-eight hours after transfection, cells were lysed in CHAPS buffer and a co-IP of NTE-GFP (182 kDa) and Myc-ARA54 (54 kDa) was performed using an anti-GFP monoclonal antibody. The co-immunoprecipitated NTE-GFP was detected by Western blotting using an anti-Myc monoclonal antibody. (B) The cotransfected COS7 cell lysates were immunoprecipitated by anti-Myc antibody and then detected by Western blotting using anti-GFP antibody. (C) Colocalization of NTE-GFP and ARA54-DsRed in transfected COS7 cells. Cells were transiently cotransfected with NTE-GFP or GFP and ARA54-DsRed constructs; 48 h post-transfection cells were fixed, and the distribution of fluorescent proteins was analyzed by confocal microscopy. The bar is 10 μm. (D) HeLa cell lysates were immunoprecipitated by either anti-NTE or control antibody (normal mouse IgG), and the immunoprecipitated products were detected by Western blotting with anti-ARA54 antibody.
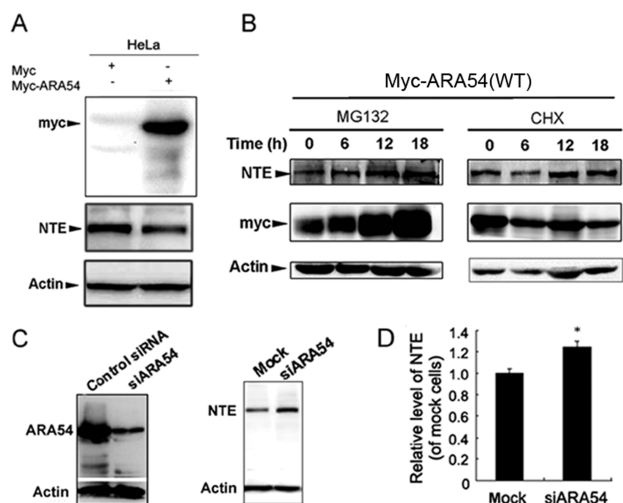
Figure 6. ARA54 regulates the NTE protein level. (A) HeLa cells were transfected with Myc-ARA54 or Myc (as a control). Forty-eight hours after transfection, total cell lysates were used to detect the expression of Myc-ARA54 (54 kDa) and NTE (155 kDa) by Western blotting. Actin (42 kDa) was used as a loading control. The blots shown are representative of three independent experiments. (B) HeLa cells were transfected with Myc-ARA54 (WT). Twenty-four hours after transfection, cells were treated with 20 μM MG132 or 30 μM cycloheximide (CHX) for the indicated time. Total cell lysates were analyzed by immunoblotting using anti-NTE antibody. Actin was used as a loading control. (C) Western blotting data show the endogenous ARA54 level (left) and NTE level (right) in siARA54 and control siRNA (mock)-transfected HeLa cells. Actin was used as a loading control. (D) The relative level of NTE was quantified by densitometry. Data are presented as means ± SE ($n = 3$). *$P < 0.05$.

ARA54 expression (compare to Figure 2). These results indicate that ARA54 regulates NTE at the post-translational level.

To demonstrate that endogenous ARA54 can function as a regulator of NTE, we used siRNA to silence endogenous ARA54 expression in HeLa cells. Consistent with previous work, ARA54 expression was significantly suppressed by ARA54 siRNA (siARA54) compared with the control siRNA (Figure 6C). The level of expression of NTE was increased 0.25-fold by the knockdown of ARA54 (Figure 6D), which indicated reduction of ARA54 inhibited the degradation of NTE and ARA54 was involved in the regulation of NTE protein levels.

A previous study showed that ARA54 had autoubiquitination activity that is dependent on the RING-finger domain (RING), which is responsible for the interaction with a Ub-conjugating enzyme.[27] To investigate whether ARA54 also acts as a Ub-ligase in the degradation of NTE, we constructed a mutant ARA54 with a C220S point mutation, which results in a dysfunctional RING domain [MT ARA54 (Figure 7A)]. As shown in panels B and C of Figure 7, overexpression of WT ARA54 significantly increased the level of degradation of NTE and decreased the level of NTE. In contrast, overexpressing MT ARA54 was much less effective in decreasing the NTE level. These data indicate that the RING domain of the Ub-ligase ARA54 is critical for the degradation of NTE.

■ DISCUSSION

Degradation of cytoplasmic proteins proceeds via two pathways: the ubiquitin proteasome pathway and autophagy. Here,
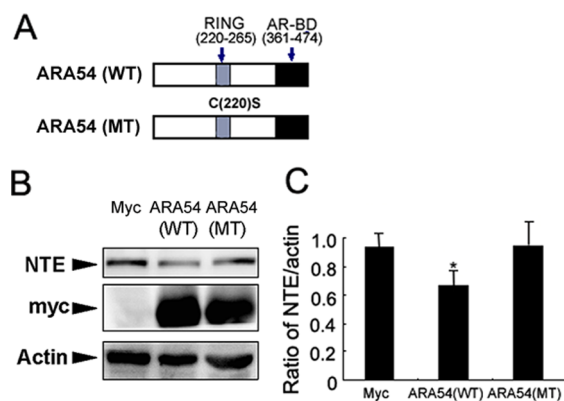

Figure 7. ARA54 regulates the NTE level by the RING-finger motif. (A) Structures of wild-type (WT) ARA54 and its RING point mutant (MT). The numbers indicate the amino acid positions. The RING is indicated as a filled gray box and the AR-BD as a filled black box. (B) Western blotting data show the endogenous NTE level in ARA54 (WT)- and ARA54 (MT)-expressing HeLa cells. Actin was used as a loading control. The myc-ARA54 (WT or MT) was 54 kDa, NTE protein 155 kDa, and actin protein 42 kDa. (C) The relative level of NTE was quantified by densitometry and is shown with the NTE:actin ratio. Data are presented as means ± SE ($n = 3$). *$P < 0.05$.

using inhibitors of proteasomal degradation, we showed that both the overexpressed and endogenous NTE are degraded by the proteasome pathway. Furthermore, co-immunoprecipitation experiments showed that NTE protein can be ubiquitinated.

The D-box (consensus RXXLXXXXN sequence) is a known recognition signal found in substrates that are degraded by the UPP.[16] The D-box was originally identified as a conserved nine-amino acid motif in sea urchin cyclin B.[15] The consensus for the motif in B-type cyclins is RXALGXIXN, in which R at position 1 and L at position 4 are highly conserved except for that of cyclin B3, which has F instead of L at position 4.[28] Mutations in the D-box of cyclin B prevented its ubiquitination and proteolysis.[15] Preliminary bioinformatics analysis showed that there is a similar sequence (RVTFLALHN, residues 276−284) within the R domain of NTE to the D-box of cyclin B3. Thus, we propose that the D-box of NTE may act as recognition signal for NTE degradation. Our results showed that only NTER, but not ΔR-NTE or NTEC, tagged with GFP accumulated after treatment with MG132. These results indicate that the R domain of NTE contributes to NTE degradation by UPP. However, further studies are required to determine whether these residues in the D-box affect the degradation of NTE. We previously identified an androgen receptor-associated protein ARA54 as an interacting protein with ΔTm-NTE-R by using yeast two-hybrid screening.[21] These data indicated that NTE may be degraded by the ubiquitin−proteasome pathway with ARA54.

ARA54 was first identified as a ligand-dependent interaction partner with the androgen receptor, and ARA54 could enhance the transactivation of AR.[29] The physiological roles of ARA54 in prostate cancer progression have been well studied.[22,30,31] ARA54 mRNA is expressed at the highest levels in testis but is also expressed at different levels in a variety of other human tissues, such as thymus, spleen, colon, prostate, uterus, blood leukocyte, and small intestine,[29] indicating that ARA54 may function in a manner independent of androgen-mediated signaling. Recently, ARA54 has been found to be involved in transcriptional regulation of the *cyclin D1* gene in the absence

of AR stimulation.[32] However, AR-independent functions of ARA54 are still not entirely known.

ARA54 has two protein domains: the AR-binding domain (AR-BD) and a RING domain (Figure 7A). ARA54 was demonstrated to be autoubiquitinated, and the RING domain was critical for its interaction with class III E2s, such as UBE2E2, UbcH6, and UBE2E3.[27] However, the substrate proteins of ARA54 had not been identified. Our results are the first to show that NTE is a target protein of ARA54 and ARA54 regulates NTE levels in an AR-independent manner. Moreover, the RING domain was demonstrated to be essential for the regulation of NTE by ARA54. NTE protein is also expressed in non-neuronal tissues, including testis, intestine, placenta, and lymphocytes.[4,33,34] Thus, ARA54 and NTE coexist in various tissues.

In summary, we reveal that ARA54 acts as the ubiquitin-ligase to regulate the ubiquitin−proteasome degradation of NTE. Important questions about what factors or conditions affect the exposure of the destruction box in NTE, how ARA54 gets recruited, and other factors influencing the degradation and synthesis of NTE remain to be addressed in future studies.

■ AUTHOR INFORMATION

Corresponding Author
*Institute of Zoology, CAS, 1-5 Beichenxilu Rd., Beijing 100101, P. R. China. Telephone: +86 10-64807251. Fax: +86 10 64807099. E-mail: wuyj@ioz.ac.cn.

Author Contributions
D.-X.L. and Y.-J.W. conceived and designed the experiments. D.-X.L., Y.-J.S., P.W., and R.C. performed the experiments. D.-X.L., P.W., and Y.-J.W. analyzed the data. D.-X.L., P.W., and Y.-J.W. contributed to writing of the manuscript.

Notes
The authors declare no competing financial interest.

■ ACKNOWLEDGMENTS

■ ABBREVIATIONS

3-MA, 3-methyladenine; ARA54, androgen receptor-associated protein 54; AR-BD, AR-binding domain; CHX, cycloheximide; D-box, destruction box; ER, endoplasmic reticulum; Lac, lactacystin; NTE, neuropathy target esterase; OP, organophosphorus compound; OPIDN, organophosphate-induced delayed neuropathy; PMA, phorbol 12-myristate 13-acetate; PKC, protein kinase C; TBS, Tris-buffered saline; TM, transmembrane segment; Ub, ubiquitin; UPP, ubiquitin−proteasome pathway.

■ REFERENCES

(1) Johnson, M. K. (1969) The delayed neurotoxic action of some organophosphorus compounds. Identification of the phosphorylation site as an esterase. *Biochem. J. 114*, 711−717.
(2) Johnson, M. K. (1974) The primary biochemical lesion leading to the delayed neurotoxic effects of some organophosphorus esters. *J. Neurochem. 23*, 785−789.
(3) Abou-Donia, M. B. (1981) Organophosphorus ester-induced delayed neurotoxicity. *Annu. Rev. Pharmacol. Toxicol. 21*, 511−548.
(4) Winrow, C. J., Hemming, M. L., Allen, D. M., Quistad, G. B., Casida, J. E., and Barlow, C. (2003) Loss of neuropathy target esterase in mice links organophosphate exposure to hyperactivity. *Nat. Genet. 33*, 477−485.
(5) Moser, M., Li, Y., Vaupel, K., Kretzschmar, D., Kluge, R., Glynn, P., and Buettner, R. (2004) Placental failure and impaired vasculogenesis result in embryonic lethality for neuropathy target esterase deficient mice. *Mol. Cell. Biol. 24*, 1667−1679.
(6) Akassoglou, K., Malester, B., Xu, J., Tessarollo, L., Rosenbluth, J., and Chao, M. V. (2004) Brain-specific deletion of neuropathy target esterase/swisscheese results in neurodegeneration. *Proc. Natl. Acad. Sci. U. S. A. 101*, 5075−5080.
(7) Rainier, S., Bui, M., Mark, E., Thomas, D., Tokarz, D., Ming, L., Delaney, C., Richardson, R. J., Albers, J. W., Matsunami, N., Stevens, J., Coon, H., Leppert, M., and Fink, J. K. (2008) Neuropathy target esterase gene mutations cause motor neuron disease. *Am. J. Hum. Genet. 82*, 780−785.
(8) Li, Y., Dinsdale, D., and Glynn, P. (2003) Protein domains, catalytic activity, and subcellular distribution of neuropathy target esterase in Mammalian cells. *J. Biol. Chem. 278*, 8820−8825.
(9) Quistad, G. B., Barlow, C., Winrow, C. J., Sparks, S. E., and Casida, J. E. (2003) Evidence that mouse brain neuropathy target esterase is a lysophospholipase. *Proc. Natl. Acad. Sci. U. S. A. 100*, 7983−7987.
(10) Muhlig-Versen, M., da Cruz, A. B., Tschape, J. A., Moser, M., Buttner, R., Athenstaedt, K., Glynn, P., and Kretzschmar, D. (2005) Loss of Swiss cheese/neuropathy target esterase activity causes disruption of phosphatidylcholine homeostasis and neuronal and glial death in adult *Drosophila. J. Neurosci. 25*, 2865−2873.
(11) Zaccheo, O., Dinsdale, D., Meacock, P. A., and Glynn, P. (2004) Neuropathy target esterase and its yeast homologue degrade phosphatidylcholine to glycerophosphocholine in living cells. *J. Biol. Chem. 279*, 24024−24033.
(12) Chen, R., Chang, P. A., Long, D. X., Yang, L., and Wu, Y. J. (2007) Down-regulation of neuropathy target esterase by protein kinase C activation with PMA stimulation. *Mol. Cell. Biochem. 302*, 179−185.
(13) Chen, R., Chang, P. A., Long, D. X., Liu, C. Y., Yang, L., and Wu, Y. J. (2007) G protein β2 subunit interacts directly with neuropathy target esterase and regulates its activity. *Int. J. Biochem. Cell Biol. 39*, 124−132.
(14) Long, D. X., Chang, P. A., Liang, Y. J., Yang, L., and Wu, Y. J. (2009) Degradation of neuropathy target esterase by the macro-autophagic lysosomal pathway. *Life Sci. 84*, 89−96.
(15) Glotzer, M., Murray, A. W., and Kirschner, M. W. (1991) Cyclin is degraded by the ubiquitin pathway. *Nature 349*, 132−138.
(16) Pfleger, C. M., and Kirschner, M. W. (2000) The KEN box: an APC recognition signal distinct from the D box targeted by Cdh1. *Genes Dev. 14*, 655−665.
(17) Chang, P. A., Chen, Y. Y., Qin, W. Z., Long, D. X., and Wu, Y. J. (2011) The role of cell cycle-dependent neuropathy target esterase in cell proliferation. *Mol. Biol. Rep. 38*, 123−130.
(18) Hershko, A., and Ciechanover, A. (1998) The ubiquitin system. *Annu. Rev. Biochem. 67*, 425−479.
(19) Weissman, A. (2001) Themes and variations on ubiquitylation. *Nat. Rev. Mol. Cell Biol. 2*, 169−178.
(20) Schwartz, A. L., and Ciechanover, A. (1999) The ubiquitin-proteasome pathway and pathogenesis of human diseases. *Annu. Rev. Med. 50*, 57−74.

(21) Chen, R., Yang, L., Yao, Z., Liu, C. Y., Li, X. H., Li, Q., Liu, J., Chang, P. A., Li, W., and Wu, Y. J. (2005) Hunting for novel proteins in neuropathy target esterase regulator domain with yeast two-hybrid system. *DongWuXueBao (Acta Zoologica Sinca) 51*, 840−844.

(22) Yang, Z., Chang, Y. J., Miyamoto, H., Yeh, S., Yao, J. L., di Sant'Agnese, P. A., Tsai, M.-Y., and Chang, C. (2007) Suppression of androgen receptor transactivation and prostate cancer cell growth by heterogeneous nuclear ribonucleoprotein A1 via interaction with androgen receptor coregulator ARA54. *Endocrinology 148*, 1340−1349.

(23) Lee, D. H., and Goldberg, A. L. (1998) Proteasome inhibitors: valuable new tools for cell biologists. *Trends Cell Biol. 8*, 397−403.

(24) Nostrandt, A. C., and Ehrich, M. (1992) Development of a model cell culture system in which to study early effects of neuropathy-inducing organophosphorus esters. *Toxicol. Lett. 60*, 107−114.

(25) Tsien, R. Y. (1998) The green fluorescent protein. *Annu. Rev. Biochem. 67*, 509−544.

(26) Verkhusha, V. V., and Lukyanov, K. A. (2004) The molecular properties and applications of Anthozoa fluorescent proteins and chromoproteins. *Nat. Biotechnol. 22*, 289−296.

(27) Ito, K., Adachi, S., Iwakami, R., Yasuda, H., Muto, Y., Seki, N., and Okano, Y. (2001) N-Terminally extended human ubiquitin-conjugating enzymes (E2s) mediate the ubiquitination of RING-finger proteins, ARA54 and RNF8. *Eur. J. Biochem. 268*, 2725−2732.

(28) Yamano, H., Tsurumi, C., Gannon, J., and Hunt, T. (1998) The role of the destruction box and its neighbouring lysine residues in cyclin B for anaphase ubiquitin-dependent proteolysis in fission yeast: defining the D-box receptor. *EMBO J. 17*, 5670−5678.

(29) Kang, H. Y., Yeh, S., Fujimoto, N., and Chang, C. (1999) Cloning and characterization of human prostate coactivator ARA54, a novel protein that associates with the androgen receptor. *J. Biol. Chem. 274*, 8570−8576.

(30) Miyamoto, H., Rahman, M., Takatera, H., Kang, H. Y., Yeh, S., Chang, H. C., Nishimura, K., Fujimoto, N., and Chang, C. (2002) A dominant-negative mutant of androgen receptor coregulator ARA54 inhibits androgen receptor-mediated prostate cancer growth. *J. Biol. Chem. 277*, 4609−4617.

(31) Yang, Z., Chang, Y. J., Miyamoto, H., Ni, J., Niu, Y., Chen, Z., Chen, Y. L., Yao, J. L., di Sant'Agnese, P. A., and Chang, C. (2007) Transgelin functions as a suppressor via inhibition of ARA54-enhanced androgen receptor transactivation and prostate cancer cell growth. *Mol. Endocrinol. 21*, 343−358.

(32) Kikuchi, H., Uchida, C., Hattori, T., Isobe, T., Hiramatsu, Y., Kitagawa, K., Oda, T., Konno, H., and Kitagawa, M. (2007) ARA54 is involved in transcriptional regulation of the cyclin D1 gene in human cancer cells. *Carcinogenesis 28*, 1752−1758.

(33) Williams, D. G. (1983) Intramolecular group transfer is a characteristic of neurotoxic esterase and is independent of the tissue source of the enzyme. A comparison of the aging behaviour of di-isopropyl phosphorofluoridate-labelled proteins in brain, spinal cord, liver, kidney and spleen from hen and in human placenta. *Biochem. J. 209*, 817−829.

(34) Schwab, B. W., and Richardson, R. J. (1986) Lymphocyte and brain neurotoxic esterase: dose and time dependence of inhibition in the hen examined with three organophosphorus esters. *Toxicol. Appl. Pharmacol. 83*, 1−9.